IEEE Access
Multidisciplinary ⋮ Rapid Review ⋮ Open Access Journal

Received August 6, 2019, accepted September 3, 2019, date of publication September 12, 2019,
date of current version September 25, 2019.

Digital Object Identifier 10.1109/ACCESS.2019.2941118

Prediction Method of Concentricity and Perpendicularity of Aero Engine Multistage Rotors Based on PSO-BP Neural Network

CHUANZHI SUN, CHENGTIAN LI, YONGMENG LIU, ZEWEI LIU, XIAOMING WANG, AND JIUBIN TAN

[1]Center of Ultra-Precision Optoelectronic Instrument Engineering, Harbin Institute of Technology, Harbin 150080, China
[2]Key Laboratory of Ultra-Precision Intelligent Instrumentation Engineering, Ministry of Industry and Information Technology, Harbin Institute of Technology, Harbin 150080, China

Corresponding author: Yongmeng Liu (lym@hit.edu.cn)

This work was supported in part by the National Natural Science Foundation of China under Grant 51805117, in part by the Fundamental Research Funds for the Central Universities under Grant HIT.NSRIF.2019019, in part by the China Postdoctoral Science Foundation under Grant 2019M651279, in part by the Heilongjiang Postdoctoral Fund under Grant LBH-Z18078, and in part by the Equipment Pre-Research Field Foundation under Grant 61400030401.

ABSTRACT This paper proposes a method for predicting concentricity and perpendicularity based on PSO-BP neural network in order to solve the problem of low accuracy for aero engine multistage rotors assembly. The influence factors of error propagation in the assembly are analyzed based on the characteristics of rotor structure and assembly process. And neural networks for predicting concentricity and perpendicularity of multistage rotors assembly are established. The particle swarm algorithm is used to optimize the hyperparameters of the neural network and the optimal hyperparameters can be obtained. In order to verify the effectiveness of the concentricity and perpendicularity prediction method proposed in this paper, experiments are carried out for four rotors assembly with precision rotary measuring instrument. The results show that for the 30 groups of testing samples, the average deviations of concentricity and perpendicularity by PSO-BP neural network prediction method are 1.0 μm and 0.6 μm, respectively. The prediction accuracy of concentricity and perpendicularity of final assembly are improved by 4.5 μm and 2.6 μm, respectively, compared with the traditional assembly method. The proposed method in this paper can be used not only for the guidance of multistage rotors assembly of aero engine, but also for the tolerance allocation in the design process.

INDEX TERMS PSO-BP neural network, concentricity, perpendicularity, rotor, assembly.

I. INTRODUCTION

In the field of advanced aero engine manufacturing, the quality of precise multistage rotors assembly has an important impact on the rotation quality [1], [2]. The concentricity and perpendicularity are the key parameters to evaluate the assembly quality of multistage rotors. They affect not only the radial and axial contact friction characteristics, but also the vibration characteristics at high rotation speed [3], [4]. The concentricity and perpendicularity of each rotor are propagated and accumulated in the assembly, which may lead to the concentricity and perpendicularity exceed the alarm limits and even cause the machine failure [5], [6]. For example, the concentricity and perpendicularity of final assembly must be controlled within 40 μm and 20 μm respectively for multistage rotors assembly of advanced aero engine [7], [8].

For multistage components assembly, scholars have done a lot of research on the error propagation to ensure that the parameters of final assembly meet the performance requirements [9], [10]. The homogeneous 4×4 matrix transforms were used to describe the error propagation process [11]. Mantripragada et al. proposed an error transfer algorithm based on the state transition model for mechanical assembly, which considers model environment, statistical control theory and fixture to control error transfer step by step [12]. Wang et al. proposed a stack-build assembly technique, which analyzes the location and orientation tolerances propagation process in the assembly, and the cumulative eccentric deviations can be minimized by controlling the assembly angle of each component, which reduces the eccentric deviation in cylindrical components assembly by nearly

The associate editor coordinating the review of this manuscript and approving it for publication was Okyay Kaynak.

50% [13]. In order to improve the assembly efficiency, the intelligent optimization methods were used for the multistage rotors [14]–[17]. Huang et al. utilized the multi-island genetic algorithm (MIGA) to optimize two-disk rotor system. The optimization method found the optimum rotor positions of the flexible rotor system which resulted in minimum vibration amplitudes [18]. Xi et al. proposed the least squares support vector machine for class imbalance learning for solving classification problem on balanced datasets, and the proposed algorithm can be selected as candidate techniques for fault detection of aircraft engine [19]. Choi et al introduced immune system capability into genetic algorithm to optimize rotor-bearing systems with dynamic constraints and proposed combined optimization algorithm (immune-genetic algorithm), which can reduce the transmission force between rotor and bearing [20].

Based on the references mentioned above, it can be seen that the geometric error propagation and optimization methods have been established in the assembly of multistage rotors. However, in the multistage rotors assembly, the rotors are connected by a great number of bolts with high strength and the irregular geometric deformations on the surface of bolt connection caused by the uneven tightening torque of the bolt group is not taken into account, which results in a big error between the prediction result obtained by the model and the actual result. Due to the relationship between the tightening force of the bolt group and the geometric deformation of final assembly is very complex and has not been obtained. The prediction method of concentricity and perpendicularity for the multistage rotors assembly has not been established, which takes both tightening torque and geometric errors into account. The neural network method provides a mathematical model for regression fitting and the mapping function from input to output can be obtained. Moreover, the feature of nonlinear mapping in neural network is suitable for solving problems with complex internal mechanisms [21]–[23]. In order to improve the efficiency of hyperparameters optimization, particle swarm is used to optimize BP neural network. And the proposed PSO-BP neural network method can improve the prediction accuracy of concentricity and perpendicularity for the multistage rotors assembly.

The rotor structure characteristics and the assembly process are analyzed in section 2. In section 3, the BP neural network for the prediction of concentricity and perpendicularity is established, which takes the geometric errors of each rotor and tightening torque as inputs and the concentricity and perpendicularity of final assembly as outputs respectively. The particle swarm algorithm is used to optimize the hyperparameters of the neural network. The assembly strategy for multistage rotors is established in section 4. In section 5, the effectiveness of the PSO-BP neural network prediction method is verified by the precision rotary measuring instrument in four rotors assembly. The experimental results show that the average deviation and the standard deviation of concentricity of final assembly using PSO-BP neural network are 1.0 μm and 0.7 μm, respectively.

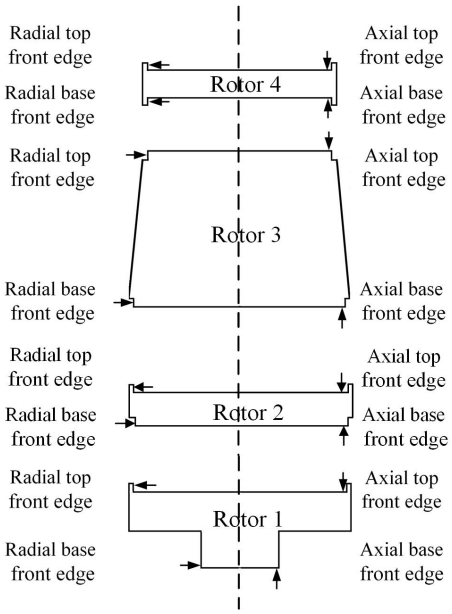

FIGURE 1. Schematic diagram of four rotors assembly.

And the average deviation and the standard deviation of perpendicularity are respectively 0.6 μm and 0.4 μm. Compared with the traditional assembly strategy, the prediction accuracy of concentricity and perpendicularity average deviations of four rotors assembly using PSO-BP neural network assembly strategy are improved by 4.5 μm and 2.6 μm, respectively.

II. THE ANALYSIS ON ERROR SOURCE OF THE MULTISTAGE ROTORS ASSEMBLY

As shown in Fig. 1, the multistage rotors are fitted by radial and axial front edges and are locked by bolts on the rotor connection surface. For example, the radial and axial top front edges of rotor 1 are fitted with the radial and axial base front edges of rotor 2 respectively and are locked by bolts on the connection surface between rotor 1 and rotor 2.

As shown in Fig. 2, O is the center of the base surface of rotor 1, and the rotation axis passes the point O and is perpendicular to the base surface. O_1, O_2, O_3 and O_4 are the geometric centers of rotors 1, 2, 3 and 4, respectively. The concentricity of the rotor is twice of its eccentricity error. And the concentricity and perpendicularity are propagated and amplified through the connection surface in the assembly. The concentricity and perpendicularity of final assembly can be reduced by controlling the assembly angle of each rotor.

As shown in Figs. 1 and 2, the concentricity and perpendicularity of final assembly using traditional stack-build assembly method [13] can be given by

$$\begin{aligned} \boldsymbol{dp}_{0-n} &= \begin{bmatrix} dx_{0-n} \\ dy_{0-n} \\ dz_{0-n} \end{bmatrix} \\ &= \sum_{i=1}^{n} \left(\prod_{j=2}^{i} \left(\boldsymbol{R}_{rj-1} \boldsymbol{R}_{xj-1} \boldsymbol{R}_{yj-1} \right) \boldsymbol{R}_{ri} \left(\boldsymbol{p}_i + \boldsymbol{dp}_i \right) \right) \end{aligned} \quad (1)$$

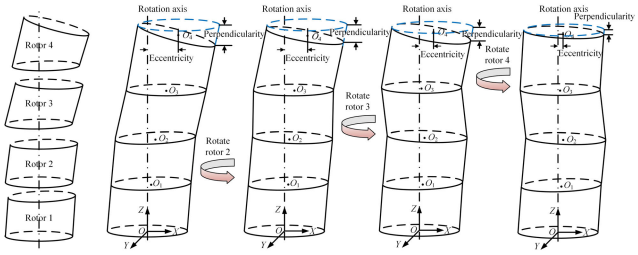

FIGURE 2. Four rotors assembly model with orientations favorable for reducing concentricity and perpendicularity.

where $\boldsymbol{dp}_{0-n}$ is the geometric center position vector in n rotors assembly. dx_{0-n}, dy_{0-n}, and dz_{0-n} are the geometric center positions of final assembly in the X, Y and Z directions, respectively. $\boldsymbol{R}_{ri}$ is the assembly rotation matrix of the ith rotor. $\boldsymbol{R}_{xj}$ and $\boldsymbol{R}_{yj}$ are the rotation matrices of the connection surfaces about the X and Y axes for the ith rotor, respectively. $\boldsymbol{p}_i$ and $\boldsymbol{dp}_i$ are the nominal position and position error vectors of the ith rotor, respectively. The concentricity and perpendicularity of final assembly are $2\sqrt{dx_{0-n}^2 + dy_{0-n}^2}$ and $2\left(dz_{0-n} - \sum_{i=1}^{n} z_i\right)$, respectively. And z_i is the height of each rotor, which includes the ideal height and the height processing error, $i = 1, 2, \ldots, n$. Due to height processing error is far less than ideal height, the concentricity and perpendicularity of final assembly caused by the height processing error can be negligible. And the radius of each rotor also has the similar characteristic.

Equation (1) shows that the concentricity and perpendicularity of final assembly are affected by the matrices $\boldsymbol{R}_{ri}$, $\boldsymbol{R}_{xj}$, $\boldsymbol{R}_{yj}$ and the vectors $\boldsymbol{p}_i$ and $\boldsymbol{dp}_i$, which related to the height, radius, eccentricity, eccentric angle, perpendicularity, the lowest point angle and assembly angle of each rotor. In addition, the tightening torque is also an important error source in the assembly.

A. GEOMETRIC ERRORS

The geometric errors of each rotor are shown in Fig. 3. O' is the geometric center, O is the rotation center, e is the eccentricity, θ_e is the eccentric angle, h is the perpendicularity, and θ_l is the lowest point angle of the connection surface. The eccentricity is caused by the inconsistency between the geometric center and the rotation center and the perpendicularity is caused by the inconsistency between the rotation axis and the normal line of the connection surface. The eccentricity and perpendicularity will be propagated and amplified through the connection surface in the assembly. And the eccentric angle and the lowest point angle point to the error propagation directions, respectively. The eccentricity and perpendicularity cannot be completely avoided by precision machining.

In addition, for a certain type of aero engine, the height and radius of each rotor are fixed and the concentricity and perpendicularity of final assembly caused by the height and radius processing errors can be negligible. Therefore, the network is established without considering the influence of the height and radius of the rotor on the concentricity and perpendicularity of final assembly in this paper.

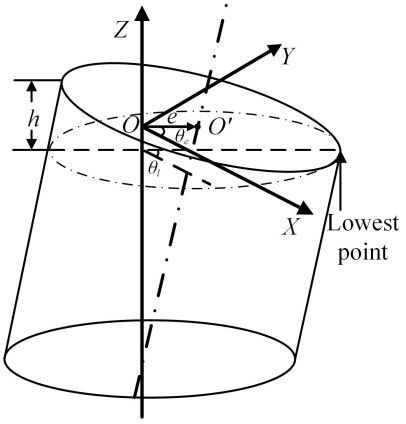

FIGURE 3. Geometric errors of the rotor.

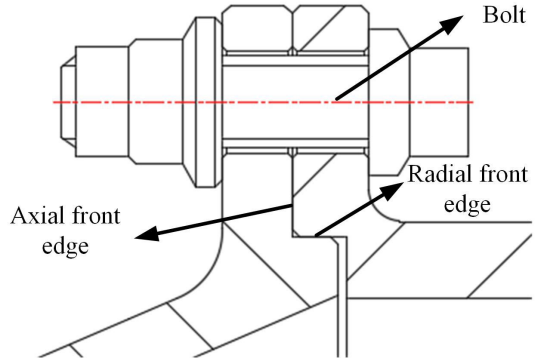

FIGURE 4. Schematic diagram of bolt tightening.

B. TIGHTENING TORQUE

The multistage rotors are connected by a great number of bolts and the way of connection can be seen in Fig. 4. In the assembly, tightening a large number of bolts would lead to the poor consistency of tightening torque and assembly repeatability. Due to the lack of the standard procedure technology of bolt tightening for multistage rotors assembly, the uniformity of tightening torque of bolt group can cause irregular geometry deformation on the bolt connection surface of the rotors, which affects the concentricity and perpendicularity of final assembly. And this error cannot be completely avoided by precision adjustment.

III. DESIGN OF PSO-BP NEURAL NETWORK

A. BP NEURAL NETWORK

There is a complex nonlinear relationship between the concentricity and perpendicularity of final assembly and the influencing factors. The concentricity and perpendicularity of final assembly are predicted using neural network in this paper because it is suitable for nonlinear fitting regression. The concentricity and perpendicularity are affected by eccentricity, eccentric angle, perpendicularity, the lowest point angle, assembly angle and tightening torque. In this paper,

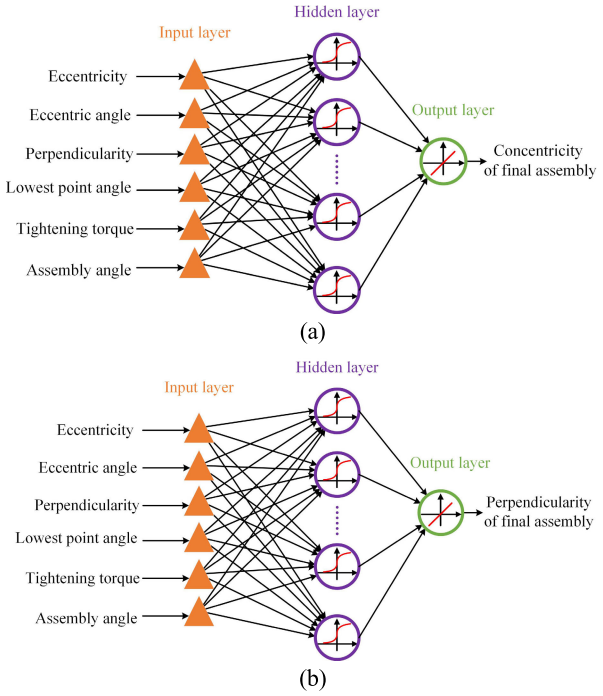

FIGURE 5. Structure of BP neural network: (a) Concentricity prediction method; (b) Perpendicularity prediction method.

the neural network for the prediction of concentricity and perpendicularity are established and the structures are shown in Figs. 5(a) and (b), respectively.

The BP neural network includes forward propagation and backward propagation. The gradient descent method is used to continuously adjust the weights and biases of the network through backward propagation, so as to minimize the mean square error (MSE) of the network. As shown in Fig. 5, the concentricity and perpendicularity prediction methods are all three-layer neural networks, namely input layer, hidden layer and output layer. As shown in equations (2) and (3), the Sigmoid function and Identity function are selected as the activation functions in the hidden layer and output layer, respectively. The mean square error (MSE) is chosen as the cost function as shown in equation (4). y_i is the actual value of the ith data, y_i' is the predicted value of ith data by the neural network, and n is the number of samples.

$$f(z) = \frac{1}{1+e^{-z}} \tag{2}$$

$$f(z) = z \tag{3}$$

$$C_0 = \frac{\sum_{i=1}^{n} (y_i - y_i')^2}{n} \tag{4}$$

The output of the prediction network is respectively the concentricity and perpendicularity of final assembly, so the number of nodes in the output layer is one. And the number of nodes in the input layer is determined by the influence factors. The learning factor and the number of hidden layer nodes will affect the learning quality of the BP neural network. If the learning factor is small, there will be the extremely slow learning speed of neural network, which increases the number of iterations and the training time. If the learning factor is large, the network will easily cross over the global optimal solution. Besides, the number of nodes in the hidden layer determines the nonlinearity of the network. If the number of nodes is small, the network is under-fitting and the large number of nodes will lead to the overfitting when the nonlinearity of the network is higher than that of the model itself. In order to avoid the overfitting problem, the L2 regularization adds a regularization term in the cost function to optimize the neural network as shown in equation (5).

$$C = C_0 + \frac{\lambda}{2n} \sum_{w} w^2 \tag{5}$$

where C is the cost function with L2 regularization, w is the connection weight of network neurons and λ is the regularization factor. If λ is small, the overfitting still exists in the network. If λ is large, the cost function will decrease rapidly and the network training will be insufficient. Therefore, the selection of the number of nodes in the hidden layer, learning factor and L2 regularization factor will be the focus of BP neural network hyperparameters adjustment.

B. PSO-BP NEURAL NETWORK

The method of controlling variables is used to determine the size of each parameter one by one in the hyperparameters optimization for the traditional BP neural network. Although the network trained by this method also has high accuracy, the calculation process is too complicated and the selected parameters are not optimal. In order to further simplify the training process and obtain the best hyperparameters, this paper establishes the BP neural network prediction methods based on particle swarm algorithm for hyperparameters optimization. Each particle in the algorithm represents a potential solution to the problem and the particle velocity is dynamically adjusted by the particle itself and other particles. M particles is constituted as the particle swarm in D-dimensional search space and the particle velocity and position can be expressed as:

$$v_{id}^{k+1} = uv_{id}^{k} + c_1 r_1 \left(pb_{id}^{k} - x_{id}^{k}\right) + c_2 r_2 \left(gb_{d}^{k} - x_{id}^{k}\right) \tag{6}$$

$$x_{id}^{k+1} = x_{id}^{k} + v_{id}^{k+1} \tag{7}$$

where v is the particle velocity, x is the particle position in space, pb is the historical optimum position of each particle in space, gb is the historical optimum position of the whole swarm in space, $d = [1, 2, \ldots, D]$, $i = [1, 2, \ldots, M]$, k is the number of iterations, r_1 and r_2 are random numbers between [0, 1], c_1 and c_2 are learning factors of PSO and u is inertia weight, which balances the local search ability and global search ability. $c_1 = c_2 = 2$, $u = 0.5$.

In order to obtain the number of nodes in the hidden layer, learning factor and L2 regularization factor in BP neural

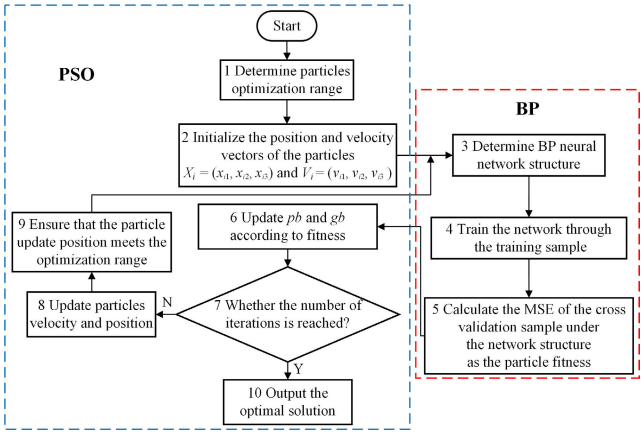

FIGURE 6. Flow chart of PSO-BP neural network.

network, a particle swarm with three-dimensional search space ($D = 3$) is established. According to the actual situation of the neural network, the number of nodes in the hidden layer should be an integer. Therefore, the particle swarm position coordinates corresponding to the hyperparameters must be kept integer when the particle swarm position is initialized and updated. The BP neural network flow chart based on particle swarm algorithm for hyperparameters optimization is shown in Fig. 6.

As shown in Fig. 6, the training process of PSO-BP is as follows:

Step 1: Determine the optimization range of each hyperparameter, including the number of nodes in the hidden layer, learning factor and L2 regularization factor.

Step 2: Initialize the particle swarm according to the optimization range and the space position corresponding to the number of nodes in the hidden layer is guaranteed to be an integer.

Step 3: The hyperparameters of each particle in the particle swarm are substituted into the BP neural network to determine the network structure.

Step 4: Train the network by training sample to determine the weights and biases of the network.

Step 5: The validation sample is substituted into the trained network and the MSE of the validation sample is calculated. The MSE is used as the particle fitness.

Step 6: The historical optimum position of each particle in space *pb* and the historical optimum position of the whole swarm in space *gb* are updated according to fitness.

Step 7: Determine whether the maximum number of iterations has been reached.

Step 8: If the maximum number of iterations is not reached, the velocity and position of particles are updated by equations (6) and (7).

Step 9: In order to guarantee that the obtained particle position can be used to determine the BP neural network hyperparameters, it is necessary to ensure that the particle position conforms to the optimization range. Repeat steps 3-7.

Step 10: If the maximum number of iterations is reached, the historical optimum position of each particle in space *pb* can be output and the optimal hyperparameters of the network can be obtained.

IV. ASSEMBLY STRATEGY

The constrained nonlinear programming is the optimization of objective functions with equality or inequality constraints. The concentricity and perpendicularity are limited to less than a fixed value and the assembly angles are limited by the number of bolt holes in the assembly. For example, if the number of bolt holes is 18, the assembly angle is an equal interval of 20°. The optimal assembly strategy aims to obtain the best possible assembly results of final assembly, which meets the positions of bolt holes and the limits of the concentricity and perpendicularity. The optimal assembly strategy of multistage rotors based on PSO-BP neural network prediction method is shown in equation (8).

$$\begin{aligned} & f^{BP}(\theta_{rk}) \\ & = \min\left\{\max\left(\frac{c^{BP}(\theta_{rk})-c^{BP}_{\min}}{c^{BP}_{\max}-c^{BP}_{\min}}, \frac{p^{BP}(\theta_{rk})-p^{BP}_{\min}}{p^{BP}_{\max}-p^{BP}_{\min}}\right)\right\} \\ & \text{sub.to} \begin{cases} c^{BP}(\theta_{rk}) \le c_{limit} \\ p^{BP}(\theta_{rk}) \le p_{limit} \\ \theta_{rk} = 0, \dfrac{360}{t_k}, \ldots, 360-\dfrac{360}{t_k} \end{cases} \end{aligned} \tag{8}$$

where c_{limit} and p_{limit} are the limit values of concentricity and perpendicularity of final assembly, respectively. $c^{BP}_{\max}$, $c^{BP}_{\min}$, $p^{BP}_{\max}$, $p^{BP}_{\min}$ are the maximum concentricity, minimum concentricity, maximum perpendicularity, minimum perpendicularity of final assembly by PSO-BP neural network prediction method, respectively. θ_{rk} is the assembly angle of the kth rotor, t_k is the number of bolt holes of the kth rotor, $k = 1, 2, \ldots, n$. In order to further analyze the advantages of the proposed method, it is compared with the traditional analyzed method. The optimal assembly strategy based on the traditional stack-build prediction model [13] is shown in equation (9).

$$\begin{aligned} & f^{TM}(\theta_{rk}) \\ & = \min\left\{\max\left(\frac{c^{TM}(\theta_{rk})-c^{TM}_{\min}}{c^{TM}_{\max}-c^{TM}_{\min}}, \frac{p^{TM}(\theta_{rk})-p^{TM}_{\min}}{p^{TM}_{\max}-p^{TM}_{\min}}\right)\right\} \\ & \text{sub.to} \begin{cases} c^{TM}(\theta_{rk}) \le c_{limit} \\ p^{TM}(\theta_{rk}) \le p_{limit} \\ \theta_{rk} = 0, \dfrac{360}{t_k}, \ldots, 360-\dfrac{360}{t_k} \end{cases} \end{aligned} \tag{9}$$

where $c^{TM}_{\max}$, $c^{TM}_{\min}$, $p^{TM}_{\max}$, $p^{TM}_{\min}$ are respectively the maximum concentricity, minimum concentricity, maximum perpendicularity, minimum perpendicularity of final assembly by traditional stack-build prediction method.

V. EXPERIMENTS

In order to verify the effectiveness of the proposed PSO-BP neural network prediction method, experiments are carried out with precision rotary measuring instrument as shown

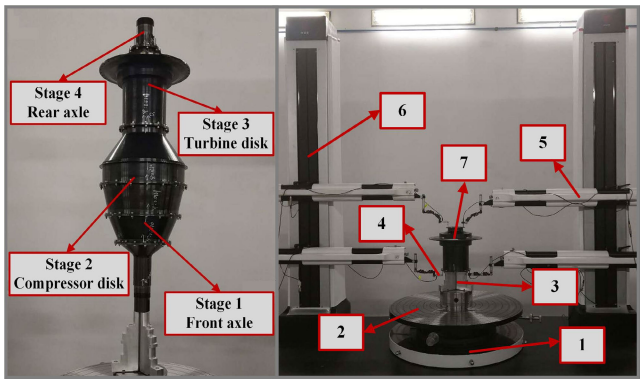

FIGURE 7. Photograph of experiment set-up: (a) Four rotors assembly; (b) Rotary measuring instrument.

TABLE 1. Geometry parameters of each rotor.

Measurement parameters	Rotor No.			
	Front axle	Compressor disk	Turbine disk	Rear axle
Height (mm)	459	35	325	76
Radius of top surface (mm)	198	109	66	40
The number of bolt holes on the top surface	36	24	18	/

in Fig. 7. The four rotors of final assembly are shown in Fig. 7(a) and the geometry parameters of each rotor are shown in Table 1. The assembly sequence of four rotors is front axle, compressor disk, turbine disk and rear axle. The concentricity and perpendicularity of final assembly are measured by the rotary measuring instrument as shown in Fig. 7(b) and the parameters of each core unit are shown as follows:

(1) Air-bearing turntable is used to provide the rotary measurement datum. The radial and axial accuracy of air-bearing turntable are 80 nm.

(2) Centering and tilt worktable is used for adjusting the eccentricity and tilt of base surface of the rotors to make the geometric axis coincident with the rotation axis. The minimum adjustment of displacement and angle are 0.2 μm and 0.2″, respectively.

(3) The chuck is used to fix the rotor.

(4) The inductive sensors are used to collect the radial and axial surface data of the rotors, which the resolutions are 0.1 μm.

(5) The displacement of the horizontal guide rail is 800 mm.

(6) The displacement of the vertical guide rail is 2000 mm.

(7) The turbine disk is the measured rotor.

In order to predict the concentricity and perpendicularity of four rotors assembly, the 300 samples are divided into training samples, validation samples and testing samples according to 8:1:1. The factors of the samples include eccentricity, eccentric angle, perpendicularity, the lowest point

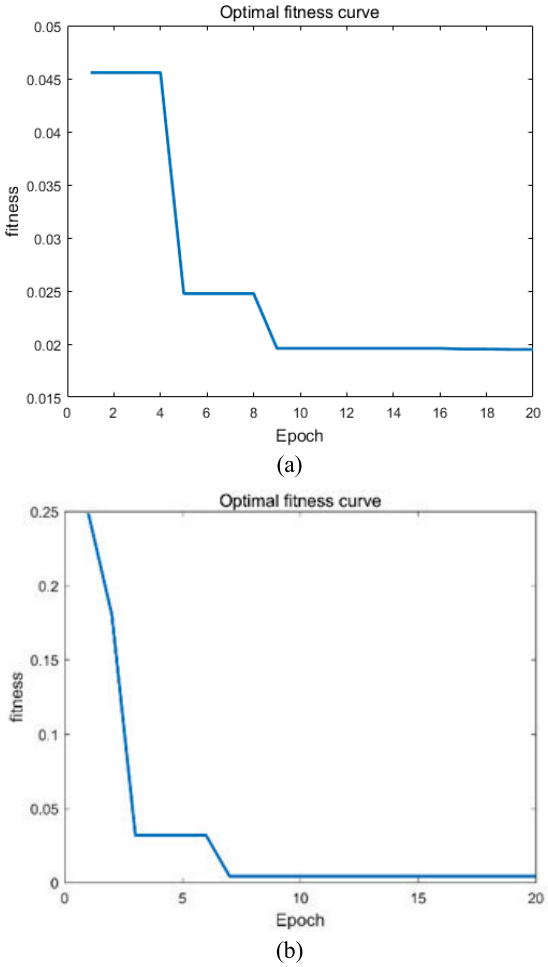

FIGURE 8. Particle swarm optimization fitness curve: (a) Concentricity prediction network; (b) Perpendicularity prediction network.

angle, assembly angle, tightening torque of each rotor and concentricity and perpendicularity of final assembly. The range of tightening torque is [14, 16] N · m and it fits the random distribution. The number of nodes in the input layer is 22 when the concentricity and perpendicularity of four rotors assembly are predicted. The optimization range of hyperparameters of the two networks is the same. The number of nodes is [25, 60] in the hidden layer. The range of learning factor is [0.0001, 0.1] and the logarithm of the scale is taken as $[-4, -1]$ in order to ensure that the scale is evenly distributed. The range of regularization factor is [0.0001, 0.01] and its logarithm is $[-4, -2]$. The number of particle swarm is 20 and the number of iterations is 20. The optimal fitness curves of particle swarm of concentricity and perpendicularity prediction methods are obtained respectively as shown in Figs. 8(a) and (b).

As shown in Fig. 8, with the increase of iterations, the optimal solution of particle swarm keeps improving. The global optimal solutions of concentricity and perpendicularity prediction methods are [48, 0.038, 0.005] and [45, 0.015, 0.004]. That means that the number of nodes is 48 in the hidden layer, learning factor is 0.038 and L2 regularization

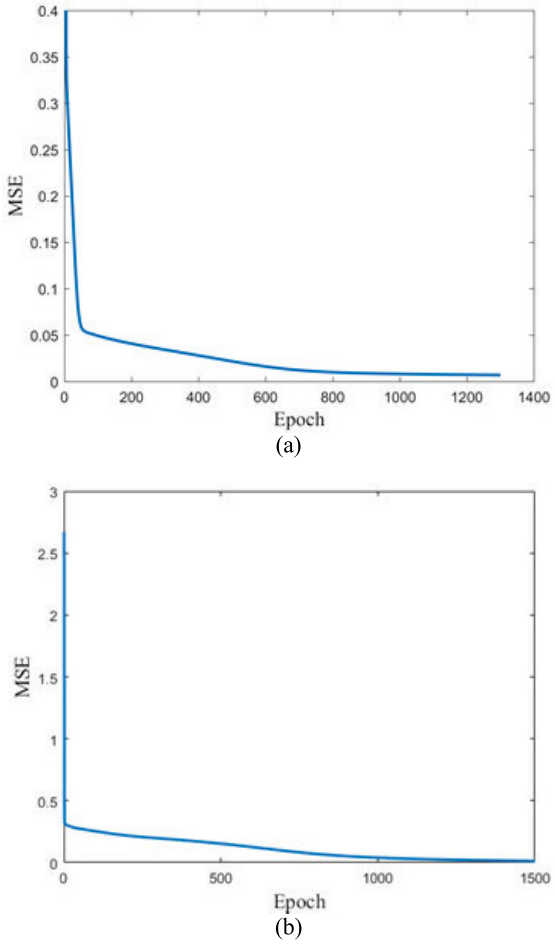

FIGURE 9. The MSE of validation sample: (a) Concentricity prediction network; (b) Perpendicularity prediction network.

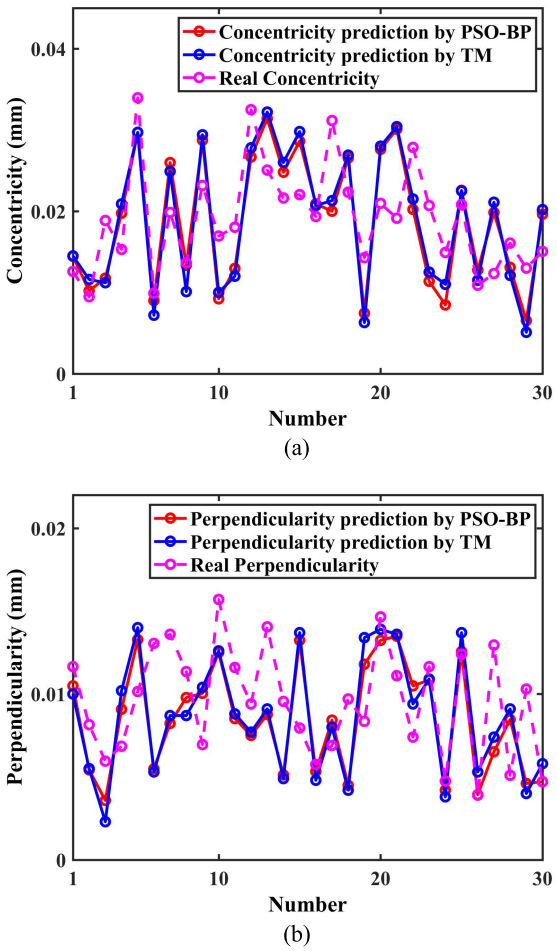

FIGURE 10. Experimental results: (a) Concentricity prediction results; (b) Perpendicularity prediction results.

factor is 0.005 for the concentricity prediction network of four rotors assembly. And the number of nodes is 45 in the hidden layer, learning factor is 0.015 and L2 regularization factor is 0.004 for the perpendicularity prediction network of four rotors assembly.

The optimal hyperparameters are used to train the prediction networks of concentricity and perpendicularity, and the MSE values of the validation samples are shown in Figs. 9(a) and (b), respectively. The MSE values of the two network validation samples are to be stable when the number of iterations reaches 1200. The performance of the network improves little with the increase of iterations and the training of concentricity and perpendicularity prediction networks is completed.

As shown in Fig. 10, the 30 groups of testing samples are tested using PSO-BP neural network assembly strategy and traditional stack-build assembly strategy, respectively. The predicted concentricity and perpendicularity of four rotors assembly using PSO-BP neural network assembly strategy are consistent with the actual trend of concentricity and perpendicularity. It verifies the effectiveness of the concentricity and perpendicularity prediction method based on PSO-BP neural network. In addition, the average deviation of concentricity prediction is 1.0 μm, the standard deviation is 0.7 μm, the minimum deviation is 0.1 μm, and the maximum deviation is 3.3 μm of four rotors assembly using PSO-BP neural network assembly strategy. Compared with the traditional assembly strategy, the prediction accuracy of concentricity average deviation and standard deviation of four rotors assembly using PSO-BP neural network assembly strategy are improved by 4.5 μm and 1.9 μm, respectively. And the average deviation of perpendicularity prediction is 0.6 μm, the standard deviation is 0.4 μm, the minimum deviation is 0.1 μm, and the maximum deviation is 1.6 μm of four rotors assembly using PSO-BP neural network assembly strategy. Compared with the traditional assembly strategy, the prediction accuracy of perpendicularity average deviation and standard deviation of four rotors assembly using PSO-BP neural network assembly strategy are improved by 2.6 μm and 1.5 μm, respectively.

VI. DISCUSSIONS AND CONCLUSIONS

A prediction method of concentricity and perpendicularity based on PSO-BP neural network is proposed in this paper to improve the assembly accuracy for concentricity and perpendicularity of multistage rotors assembly. The error sources

in the assembly are analyzed, which take geometric errors and tightening torque into account. The prediction networks for concentricity and perpendicularity of final assembly are established, in which the eccentricity, eccentric angle, perpendicularity, the lowest point angle, assembly angle and tightening torque are as input. In order to obtain the optimal values of the number of nodes in the hidden layer, learning factor and regularization factor in the neural network, the particle swarm algorithm is used to optimize the BP neural network.

In order to verify the effectiveness of the proposed method, the experiments are carried out in four rotors assembly using the precision rotary measuring instrument. The results show that the average deviation and the standard deviation of concentricity of final assembly using PSO-BP neural network are 1.0 μm and 0.7 μm, respectively. And the average deviation and the standard deviation of perpendicularity are respectively 0.6 μm and 0.4 μm. Compared with the traditional assembly strategy, the prediction accuracy of concentricity and perpendicularity average deviations of four rotors assembly using PSO-BP neural network assembly strategy are improved by 4.5 μm and 2.6 μm, respectively.

In this paper, the nonlinear relationship between the concentricity and perpendicularity of final assembly and the geometric errors and tightening torque of each rotor is obtained using the proposed method in the multistage rotors assembly. The method proposed in this paper can be used not only for guidance of multistage rotors assembly of aero engine, but also for the tolerance allocation in the design process.

ACKNOWLEDGMENT

This research was supported by the National Natural Science Foundation of China (grant number 51805117), the Fundamental Research Funds for the Central Universities (grant number HIT.NSRIF.2019019), the China Postdoctoral Science Foundation funded project (grant number 2019M651279), the Heilongjiang Postdoctoral Fund (grant number LBH-Z18078) and the Equipment Pre-Research Field Foundation (grant number 61400030401).

REFERENCES

[1] X. Kong, G. Liu, Y. Liu, and L. Zheng, "Experimental testing for the influences of rotation and tip clearance on the labyrinth seal in a compressor stator well," *Aerosp. Sci. Technol.*, vol. 71, pp. 556–567, Dec. 2017.
[2] H. Zhang, C. Zhang, Y. Peng, D. Wang, G. Tian, X. Liu, and Y. Peng, "Balancing problem of stochastic large-scale U-type assembly lines using a modified evolutionary algorithm," *IEEE Access*, vol. 6, pp. 78414–78424, 2018.
[3] F. Sanchez-Marin, V. Roda-Casanova, and A. Porras-Vazquez, "A new analytical model to predict the transversal deflection under load of stepped shafts," *Int. J. Mech. Sci.*, vols. 146–147, pp. 91–104, Oct. 2018.
[4] Z. Liu, Q. Tang, N. Liu, and J. Song, "A profile error compensation method in precision grinding of screw rotors," *Int. J. Adv. Manuf. Technol.*, vol. 100, pp. 2557–2567, Feb. 2019.
[5] B. Xin, Y. Li, J.-F. Yu, and J. Zhang, "Analysis of chaotic dynamics for aircraft assembly lines," *Assem. Automat.*, vol. 38, pp. 20–25, Feb. 2018.
[6] G. Peng, Y. Sun, and S. Xu, "Development of an integrated laser sensors based measurement system for large-scale components automated assembly application," *IEEE Access*, vol. 6, pp. 45646–45654, 2018.
[7] S. Hernández, E. Menga, P. Naveira, D. Freire, C. López, M. C. Montoya, S. Moledo, and A. Baldomir, "Dynamic analysis of assembled aircraft structures considering interfaces with nonlinear behavior," *Aerosp. Sci. Technol.*, vol. 77, pp. 265–272, Jun. 2018
[8] H. Qi, G. Xu, C. Lu, and Y. Shi, "A study of coaxial rotor aerodynamic interaction mechanism in hover with high-efficient trim model," *Aerosp. Sci. Technol.*, vol. 84, pp. 1116–1130, Jan. 2019.
[9] D. E. Whitney, O. L. Gilbert, and M. Jastrzebski, "Representation of geometric variations using matrix transforms for statistical tolerance analysis in assemblies," *Res. Eng. Des.*, vol. 6, pp. 191–210, Dec. 1994.
[10] A. Desrochers and A. Rivière, "A matrix approach to the representation of tolerance zones and clearances," *Int. J. Adv. Manuf. Technol.*, vol. 13, pp. 630–636, Sep. 1997.
[11] D. E. Whitney, *Mechanical Assemblies*. Oxford, U.K.: Oxford Univ., 2004, pp. 36–42.
[12] R. Mantripragada and D. E. Whitney, "Modeling and controlling variation propagation in mechanical assemblies using state transition models," *IEEE Trans. Robot. Autom.*, vol. 15, no. 1, pp. 124–140, Feb. 1999.
[13] L. Wang, C. Sun, J. Tan, B. Zhao, and G. Wan, "Improvement of location and orientation tolerances propagation control in cylindrical components assembly using stack-build assembly technique," *Assem. Automat.*, vol. 35, no. 4, pp. 358–366, 2015.
[14] J. B. Tan, "Error compensation technology for precision measurement," Harbin Inst. Technol., Harbin, China, Tech. Rep., 1995.
[15] T. Hussain, Z. Yang, A. A. Popov, and S. McWilliam, "Straight-build assembly optimization: A method to minimize stage-by-stage eccentricity error in the assembly of axisymmetric rigid components (two-dimensional case study)," *J. Manuf. Sci. Eng.*, vol. 133, no. 3, pp. 031014-1–031014-9, 2011.
[16] T. Y. Zhang, Z. J. Zhang, X. Jin, X. Ye, and Z. Zhang, "An innovative method of modeling plane geometric form errors for precision assembly," *Proc. Inst. Mech. Eng., B, J. Eng. Manuf.*, vol. 230, no. 6, pp. 1087–1096, 2016.
[17] G. Fu, T. Gu, H. Gao, Y. Jin, and X. Deng, "Geometric error compensation for five-axis ball-end milling by considering machined surface textures," *Int. J. Mech. Sci.*, vol. 99, pp. 1235–1248, Nov. 2018.
[18] J. Huang, L. Zheng, C. K. Mechefske, and B. Han, "Optimization design and experimental study of a two-disk rotor system based on multi-island genetic algorithm," *Int. J. Turbo Jet-Engines*, vol. 36, no. 1, pp. 1–8, 2019.
[19] P.-P. Xi, Y.-P. Zhao, P.-X. Wang, Z.-Q. Li, Y.-T. Pan, and F.-Q. Song, "Least squares support vector machine for class imbalance learning and their applications to fault detection of aircraft engine," *Aerosp. Sci. Technol.*, vol. 84, pp. 56–74, Jan. 2019.
[20] B.-K. Choi and B. S. Yang, "Multiobjective optimum design of rotor-bearing systems with dynamic constraints using immune-genetic algorithm," *J. Eng. Gas Turbines Power*, vol. 123, no. 1, pp. 78–81, 2001.
[21] T. Zhang, B. Ding, X. Zhao, and Q. Yue, "A fast feature selection algorithm based on swarm intelligence in acoustic defect detection," *IEEE Access*, vol. 6, pp. 28848–28858, 2018.
[22] B. Liang and T. Zhang, "Numerical optimization and cyber-physical-social computing for vibrations of the elliptical treadmill based on GSO-BPNN model," *IEEE Access*, vol. 6, pp. 10886–10895, 2018.
[23] Z. Li S. Jiang, and Y. Sun, "Chatter stability and surface location error predictions in milling with mode coupling and process damping," *Proc. Inst. Mech. Eng., B, J. Eng. Manuf.*, vol. 233, no. 3, pp. 686–698, 2019.